Wind Speed Estimation Using Acoustic Underwater Glider in a Near-Shore Marine Environment

Dorian Cazau, Julien Bonnel, *Member, IEEE*, and Mark Baumgartner

***Abstract*— This paper investigates the use of an acoustic glider to perform acoustical meteorology. This discipline consists of analyzing ocean ambient noise to infer above-surface meteorological conditions. The paper focuses on wind speed estimation, in a near-shore marine environment. In such a shallow water context, the ambient noise field is complex, with site-dependent factors and a variety of nonweather concurrent acoustic sources. A conversion relationship between sound pressure level and wind speed is proposed, taking the form of an outlier-robust nonlinear regression model learned with *in situ* data. This method is successfully applied to experimental data collected in Massachusetts Bay (MA, USA) during four glider surveys. An average error in wind speed estimation of 1.3 $\mathrm{m \cdot s^{-1}}$ (i.e., average relative error of 14%) over wind speed values up to 17 $\mathrm{m \cdot s^{-1}}$ is reported with this method, which outperformed results obtained with relationships from the literature. Quantitative results are also detailed on the dependence of wind speed error estimation on the environment characteristics, and on the classification performance of observations contaminated by acoustic sources other than wind. Passive acoustic-based weather systems are a promising solution to provide long-term *in situ* weather data with fine time and spatial resolutions. These data are crucial for satellite calibration and assimilation in meteorological models. From a broader perspective, this paper is the first step toward an operationalization of acoustic weather systems and their onboard embedding in underwater monitoring platforms such as gliders.**

***Index Terms*— Acoustical meteorology, coastal glider, outlier-robust regression model.**

I. Introduction

A. Context

ACOUSTICAL meteorology has been an active research field since the pioneering work of Nystuen *et al.* [1]. This discipline consists of analyzing ocean ambient noise to infer above-surface meteorological conditions such as wind speed and/or rainfall precipitation. It has been performed both with fixed hydrophones [2]–[4], and more recently with mobile acoustic platforms such as ARGO profilers [5]–[7] and free-ranging biologged marine mammals [8]. Up until now, acoustical meteorology has been mostly used in the open ocean (deep water), where the soundscape is generally dominated by weather-driven noise.

This paper is a proof of concept for measurements of above-surface wind speed from underwater glider's acoustic data collected in a coastal environment (shallow water). One major interest of gliders is to collect high-resolution profiles of physical, chemical, and biooptical variables in near-shore environments [9]. Our glider data are from the Woods Hole Oceanographic Institution, recorded in Massachusetts Bay (MS, USA) during four different campaigns between 2014 and 2016. The marine environment sampled by the glider is characterized by shallow waters (maximum water depth of 80 m) near the coast (distances from 1 to 30 km).

This near-shore environment introduces potential difficulties in the task of acoustical meteorology. Among major results of acoustical meteorology in shallow waters, Ma *et al.* [2] reported an increase up to 10 dB in geophysical sound levels between deep open-ocean and shallow freshwater locations, in comparison with Nystuen *et al.* [10]. A similar ambient noise level discrepancy of 10 dB has been measured for a given wind speed [11]–[13]. This could be attributed to the fact that the shallow water ambient noise is more affected by surface winds [2], [14]. Indeed, acoustic waves from surface wind speed propagate mostly vertically. Thus, shallow water tends to amplify acoustic energy induced by wind speed because of a stronger bottom reverberation, in comparison to open-ocean locations. Furthermore, Mathias *et al.* [15] reported that the frequency range of the wind dependence of ambient noise level is 0.1–14 kHz, while Nystuen *et al.* [3] reported a wind dependence up to 30 kHz. This difference can be attributed to the very shallow depth of the Mathias *et al.*'s study site (10 m at high tide). The large spread of wind-generated noise levels measured for the same wind speed in different sites can be attributed to the site dependence, which is a major challenge for acoustical meteorology. Acoustic propagation is the primary site-dependent factor that influences the noise level, which, in turn, is dependent on the season, water depth, sound speed, bottom reverberation, distinct vertical directivity, and wind fetch [11], [13], [16], [17]. For instance, Ramji *et al.* [13] reported that the wind-generated noise level measured in the Bay of Bengal during the summer was 8 dB smaller than

Manuscript received April 8, 2018; revised July 10, 2018; accepted July 19, 2018. Date of publication November 15, 2018; date of current version March 25, 2019. This work, including glider deployments, was supported by the National Marine Fisheries Service and the Saltonstall- Kennedy Grant Program. The work of D. Cazau was supported by Délégation Générale de l'Armement. The work of J. Bonnel was supported by in part by ENSTA Bretagne and in part by Andrew W. Mellon Foundation through the Joint Initiative Awards Fund. *(Corresponding author: Dorian Cazau.)*

D. Cazau is with ENSTA Bretagne, Lab-STICC, UMR CNRS 6285, 29806 Brest, France (e-mail: cazaudorian@outlook.fr).

J. Bonnel is with Applied Ocean Physics and Engineering Department, Woods Hole Oceanographic Institution, Falmouth, MA 02543 USA.

M. Baumgartner is with Biology Department, Woods Hole Oceanographic Institution, Falmouth, MA 02543 USA.

Color versions of one or more of the figures in this paper are available online at http://ieeexplore.ieee.org.

Digital Object Identifier 10.1109/TGRS.2018.2871422

during the winter and monsoon seasons. They attributed this difference to the sound speed profile variation. It has also been shown that the shallow water acoustic transmission is influenced by the season, and the attenuation is proportional to the frequency with a season-dependent coefficient [18]. Thus, the study on wind dependence of shallow water ambient noise necessitates the analysis of seasonal and site-specific parameters. Anthropogenic noise sources and biological sounds also have a greater influence on the soundscape than in deep waters, being either more recurrently present in a given spatial area, and/or closer to recorders.

To the best of authors' knowledge, no peer-reviewed publication exists that report results on using acoustic glider technology for meteorological applications. Nonetheless, Cauchy *et al.* [19] have validated the feasibility of estimating wind speed from glider data with an average absolute error of 2 $\mathrm{m} \cdot \mathrm{s}^{-1}$, and observed that depth-related errors marginally impacts this estimation. Furthermore, the study in [19] has used a clean acoustic scene in deep water, far from the coasts, and largely predominated by wind speed. The objectives of our study are as follows.

1) Demonstrate the feasibility of wind speed estimation in a noisy coastal environment using acoustic gliders.
2) Compare *in situ* learning of an empirical algorithm for wind speed conversion with those provided by the literature.
3) Evaluate the classification performance in identifying wind-generated versus nonwind noise snapshots.

B. Methodology Overview

As done in most studies, we have first set the initial hypothesis that our wind speed ground truth, i.e., W_{gt}, should fit the closest weather buoy from the glider trajectories. This hypothesis was later confirmed by basic correlation and root-mean-square (rms) error analysis between the different meteorological sources available. Please note that here, an actual ground truth at the glider location (i.e., within 500 m) is not available. Nonetheless, the closest *in situ* data available will be called "ground truth."

Our second step was to establish the empirical regression model that will be used for wind speed estimation. This wind speed will be called the acoustic wind speed W_{ac}. In the literature, various regression models have been used to link W_{gt} and W_{ac}, such as linear [19], logarithmic [2], [3], quadratic [20], or third-order polynomial [4]. Following the method proposed by Ma *et al.* [2, Appendix A], some papers use feature normalization to make their conversion model independent of recording sites and acquisition parameters. In this paper, we test different absolute regression models from the literature and compare them with a new one trained on our own recording site. Recognizing the fact that outliers could bias our model, we adopt a greedy optimization procedure. The objective is to remove these outliers so that the estimated W_{ac} optimally fits the ground truth W_{gt} (i.e., the linear regression equation $\mathrm{W}_{ac} \sim \mathrm{W}_{gt}$ has a slope of 1).

Eventually, our third processing step is to perform automatic identification of acoustic observations that do not fit the wind speed regression model. Although this step is necessary for an operational system of acoustical meteorology, it is usually ignored in the literature. Only a few studies have adopted a classification framework for this task. In particular, Ma *et al.* [2, Appendix B] and Nystuen *et al.* [3] proposed source identification algorithms of passing boats and rain events based on thresholding absolute sound pressure levels (SPLs) and their slopes in different frequency bands. In this paper, we compare this classification framework to a more complex one based on a larger set of audio descriptors and a support vector machine (SVM) classifier.

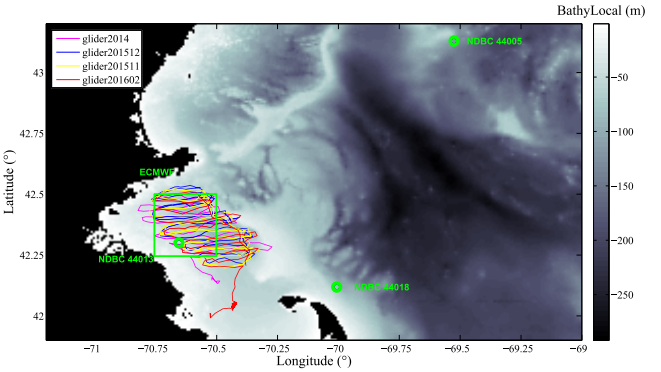

Fig. 1. Geolocalization of all glider trajectories in Massachusetts Bay (MS, USA). Glider trajectories are shown as colored trajectories. Green circles: locations of three weather buoys. Green square: ECMWF pixel used for the analysis. Local bathymetry in Massassuchetts Bay (from GEBCO-2-D, 2014) is also shown, with the color bar in meters.

II. Material and Methods

A. Measurement Sources

1) Weather Buoys: We selected three weather buoys closest to our recording area from the National Data Buoy Center,[1] namely, buoys 44005, 44013, and 44018 (see Fig. 1). These buoys are moored and equipped with a surface-mounted buoy anemometer at 10 m above the surface that provides hourly reports on wind speed. The wind speed data are, respectively, denoted as W_{44005}, W_{44013}, and W_{44018}.

We define the variable Dist_X as the time-varying Euclidean distance between the glider and the buoys X. Their respective ranges of values are: $\mathrm{Dist}_{44013} \in$ [1–24] km, $\mathrm{Dist}_{44018} \in$ [31–72] km, and $\mathrm{Dist}_{44005} \in$ [110–140] km. Naturally, weather buoys are surface contact measurements with a limited spatial monitoring area, so that distant buoys should be less interesting for our study. We further note $\mathrm{Dist} = \mathrm{Dist}_{44013}$, which is the distance between the glider and the buoy closest to the glider.

2) Model Reanalysis: The European Center for Medium-Range Weather Forecasting (ECMWF) wind speed vector was extracted from the ERA-Interim data set, based on the global atmosphere model reanalysis developed at the ECMWF. All these global reanalyses are obtained with the assimilation of a large body of different contact and satellite data. The atmospheric model is coupled to an ocean-wave model with a

[1] Website link: http://www.ndbc.noaa.gov/.

TABLE I

VARIABLES USED IN OUR STUDY, CLASSIFIED INTO THREE MEASUREMENT CATEGORIES, NAMELY, ACOUSTIC GLIDER, WEATHER BUOY, AND MODEL REANALYSIS. ALL CENTER FREQUENCIES f_c IN THE SPL AND SS DESCRIPTORS ARE ROUNDED TO A MULTIPLE OF 100 HZ FOR CLARITY IN THE NOTATION

Measurement category	Variable description	Variable label	Unit
Glider	Sound Pressure Levels (SPL) and Spectral Slopes (SS)	SPL(0.1), SPL(0.7), SPL(1.8), SPL(5), SPL(8), SPL(11), SPL(14), SPL(19), SS(2-8) and SS(8-15)	dB
	Distance between the glider and the closest buoy	Dist	m
	Depth of the glider	GliDepth	m
	Local bathymetry matched with the closest location of the glider	BathyLocal	m
	Time-varying distance between the glider and the closest land shore	DistToShore	m
Weather buoy	Wind speed from local weather buoys (NOAA-NDBC)	W_{44005}, W_{44018}, W_{44013}	$m.s^{-1}$
Model reanalysis	Wind speed from satellite data re-assimilated estimations	W_{ECMWF}	$m.s^{-1}$

TABLE II

GLOBAL OVERVIEW OF THE PASSIVE ACOUSTIC RECORDING DATA SET, WITH C BEING THE CUMULATIVE DURATION IN HOURS AND N BEING THE NUMBER OF SNAPSHOTS, ALONG WITH THE PERCENTAGE OF USEFUL SNAPSHOTS AFTER PROCESSING THE DATA

Campaigns	Time period (in date)	C (in h)	N
glider2014	01/12/2014 to 22/12/2014	31.5	9878 (87 %)
glider201511	02/11/2015 to 07/12/2015	52.6	15718 (83 %)
glider201512	07/12/2015 to 16/01/2016	60.2	18647 (86 %)
glider201602	02/02/2016 to 01/03/2016	42	12329 (81 %)
Total	-	186.3	56572 (84 %)

$1.0° \times 1.0°$ latitude/longitude grid. A detailed description of the ERA-Interim product archive can be found in [21].

The ECMWF wind speed vector is computed as $W_{ECMWF} = \sqrt{u10^2 + v10^2}$, where $u10$ and $v10$ are, respectively, the zonal and meridional wind components. Basic cleaning of the data sets is performed to remove the missing data or considered as invalid (e.g., wind speeds greater than 60 $m \cdot s^{-1}$). From $u10$ and $v10$, we compute the rms norm of the wind speed vector $W_{ECMWF} = \sqrt{u10^2 + v10^2}$. This variable has a spatial resolution of 0.25° in longitude and latitude, corresponding approximately to a 22.5 km^2 area (see pixel in Fig. 1), and a 3-h temporal resolution. Table I shows the list of these environmental variables, as well as their ranges of values.

3) Acoustic Glider:

a) Glider: Slocum coastal gliders were used (Webb Research Corporation [9]). The gliders profile in the water column by adjusting their buoyancy to become alternately heavier and lighter than the surrounding seawater. Short wings provide lift during both descent and ascent, allowing the glider to move laterally at relatively slow speeds ($\approx$0.2 $m \cdot s^{-1}$). Each glider is equipped with a global positioning system receiver to provide the vehicle's location when it is at the surface. Two-way communication with the glider is accomplished with an Iridium satellite modem. The gliders periodically surface to telemeter position, sensor, and diagnostic information so that the status of the vehicles can be monitored from land.

b) Data set: Four different campaigns conducted between 2014 and 2016 are considered in this paper. Fig. 1 provides the geolocalization of the glider trajectories in Massachusetts Bay (MS, USA). Table II provides full details of our passive acoustic recording data set. All campaigns were recorded in monophonic with a duty cycle of 1 min every 4 mins, and a sample frequency of 60 kHz (16 bytes in pulse-code modulation format). The total volume of the analyzed acoustic data set is around 300 Gb. All of the acoustic data were segmented into 10-s snapshots, and then gathered to form a single data set of independent time observations. Note that this data set is shorter than the complete original one, because of two preprocessing operations. First, roughly 15% of the data have been removed because they were near-surface observations and/or contaminated with self-generated sounds from the glider [see details in Section II-A3c)]. Second, the total number of acoustic snapshots was subset through the different Beaufort classes (nine classes from 2 $m \cdot s^{-1}$ to 20 $m \cdot s^{-1}$), and many observation snapshots occurring within the most frequent wind speed classes were randomly removed so that each of these observation subsets was balanced. Furthermore, local bathymetry is also displayed in Fig. 1, and indicates a water depth ranging from 20 to 80 m in the glider area.

c) Preprocessing: Based on the glider audio files, the following self-generated noises are identified.

1) Water splashes and swirling, characterized by short events with a broadband spectrum up to a few kilohertz.
2) Occasional activation of the rudder and buoyancy pump, characterized by a broadband spectrum up to 10–15 kHz, with higher energy in frequency bands around 1.5 and 7.5 kHz, that can last between 20 and 30 s and ending with a click.
3) Flow noise, characterized by a low-frequency broadband spectrum below 20 Hz.

These different self-generated noises are globally visible as vertical bands in a long-term averaged spectrogram. Our preprocessing simply consists of removing snapshots showing an acoustic event from one of these types. Roughly 15% of the data are removed; the exact numbers are given in Table II.

d) Acoustic features: Each 10-s snapshot is short-term fast Fourier transformed [Hamming window, 512-point fast Fourier transform (FFT), 50% overlap, yielding a 117-Hz frequency resolution], providing multiple estimates of the power spectrum levels that are subsequently averaged over 10-s snapshots via the pwelch method. Each average spectrum is then integrated on third octave frequency bands. SPL averaged over the one-third octave subband centered around f_c kHz, and the Spectral Slope (SS) between the frequencies f_1 and f_2, are extracted from the measured spectra. They are labeled SPL(f_c) and SS($f_1 - f_2$), respectively. SPLs are computed as

$$\mathrm{SPL}(f_c) = 10\log_{10}\left(\frac{1}{p_{\mathrm{ref}}^2}\sum_{f=f_{\mathrm{lower}}}^{f=f_{\mathrm{upper}}}\frac{P(f)}{B}\right) \tag{1}$$

with $f_{\mathrm{lower}} = f_c 10^{-(1/20)}$ and $f_{\mathrm{upper}} = f_c 10^{(1/20)}$, $p_{\mathrm{ref}} = 1\ \mu$Pa, and B is the noise power bandwidth of the window function ($B = 1.36$ for a Hamming window). $P(f)$ stands for the power spectral density, defined as

$$P(f) = 2\left|\frac{X(f)}{N}\right|^2 \tag{2}$$

where $X(f)$ is the FFT, given by

$$X(f) = \sum_{n=0}^{N-1} x_{\mathrm{win}}[n] e^{\frac{-i2\pi fn}{N}} \tag{3}$$

where x_{win} is a windowed segment of a time series. After correlation analysis, it appears that strong correlations exist between different pairs of SPLs close in frequency, implying that knowledge of one necessarily implies knowledge of the other. Then, to reduce the dimension of our SPL vector, we only keep the SPL(f_c) measures per octave that maximize the Pearson correlation coefficient with the variable W_{44013}.

The acoustic descriptors resulting from this process, also listed in Table I, form a 10-D feature vector over all the observations consisting of the following descriptors: SPL(0.1), SPL(0.7), SPL(1.8), SPL(5), SPL(8), SPL(11), SPL(14), SPL(19), SS(2-8), and SS(8-15). In the following, all f_c values are rounded to a multiple of 100 Hz for clarity in the notation, and all SPLs are given in dB ref μPa^2.

e) Listening area: The wind-generated acoustic energy arriving at the glider originates within a cone above the glider, with the location of the glider being the apex of the cone. Based on field results from moorings, Ma *et al.* [2, eq. 6] and Nystuen *et al.* [22] suggest that the acoustic energy arriving at a subsurface, moored hydrophone at a depth H is generated in an inverted cone with a base at the sea surface of radius nH, where n is a number between 3 and 5. We conclude that for a glider at a depth of 50 m, when neglecting refraction and absorption, 90% of the recorded acoustic signals associated with wind are originated at the sea surface inside a circle with a radius of about 500 m, centered on the position of the glider. As a result, the listening area is in the order of magnitude of a square kilometer. Wind-generated acoustic signals are, thus, associated with local wind events.

B. Characteristic Variables

We define the following variables (also displayed in Table I).

1) GliDepth as the time-varying depth of the glider. It is computed based on ambient pressure and is sampled every 4 s. Gliders followed saw-toothedlike dive profiles, with descents and ascents that last around 8 min, and with depth ranging from 0 to 60 m on average, with maximal dives up to 80 m.
2) BathyLocal as the local bathymetry matched with the closest location of the glider.
3) DistToShore as the time-varying distance between the glider and the closest land shore.

C. Statistical Processing

Prior to statistical analysis, all variables from Table I have been standardized, i.e., zero mean and unitary variance.

1) Multiple Linear Regression: Multiple Linear Regression (MLR) is a common statistical tool that informs about the linear relationship between dependent variables and independent variables. In our study, it will be used to evaluate the influence of independent variables characterizing the marine environment and recording set up on the error of wind speed estimation, i.e., the dependent variable.

To assess quantitatively the quality of our regression analysis and estimation, we provided as evaluation metrics the p-value and the multiple correlation coefficient squared (ordinary R^2, in %), also called the coefficient of determination.

2) Outlier-Robust Regression Model: In this paper, an original method based on an outlier-robust nonlinear regression model (O-R regression model) is proposed for wind speed estimation. This model is fully trained with an outlier removal procedure using *in situ* data.

a) Regression optimization: The regression model has the following second-order polynomial form that follows Pensieri *et al.* [20, eq. 4]

$$W_{ac} = a_2 * \text{SPL}(f_c)^2 - a_1 * \text{SPL}(f_c) + a_0. \tag{4}$$

As done classically in acoustical meteorology, we determine the model parameters (i.e., a_0, a_1, a_2) by least squares fitting to the sound-wind observations at the frequency f_c. Note that these parameters are not independent of each other; therefore, we iteratively search for the least squares fit by testing a range of values for each parameter.

b) Outlier removal: In statistics, Cook's distance is commonly used to estimate the influence of a data point when performing a least-squares regression analysis. In a practical ordinary least squares analysis, Cook's distance indicates influential data points that are particularly worth checking for validity. Especially, the data points with large Cook's distances correspond to large residuals (outliers) and/or to high leverages that may distort the outcome and accuracy of a regression. In our study, Cook's distance threshold is chosen through an optimization process. This distance is optimized so that the coefficient α in the regression equation $W_{ac} = \alpha \cdot W_{gt}$ tends to 1 [23]. In other words, the distance is chosen such that the estimated W_{ac} optimally fit the observations W_{gt} in each training fold.

c) Outlier classification: As explained below (Section II-C4), a 10-fold cross-validation procedure is used to assess the performance of the different models. In each fold, our O-R method learns a regression model and identifies a set of outlier observations to reject. From these 10 different sets of outliers, we selected the 2000 observations that have been the most recurrently identified as outliers. This set is labeled OutObs. Another set of observations, called WindObs, was formed by randomly selecting 2000 observations in the 10 sets of observations that fit the O-R regression model. It is assumed that WindObs data contain wind noise only, while OutObs data contain noise from other sound sources.

To identify the acoustic characteristics discriminating these two observation sets, we compute for each observation the following audio descriptors [24]:

1) *Global:* SPL(0.1), SPL(0.7), SPL(1.8), SPL(5), SPL(8), SPL(11), SPL(14), SPL(19), SS(2-8), SS(8-15), Amplitude of Energy Modulation (AmpMod);
2) *Time-Varying:* Noise Energy (NoiseErh), Spectral Skewness (SpecSkew), Spectral Kurtosis (SpecKurt), Spectro-Temporal Variation (SpecVar).

SPL and SS descriptors have been used in previous meteorological acoustic studies. In particular, SS was used to discriminate between passing ships, rainfall, and wind speed [3], [4]. The other descriptors are classical features that are used in various audio classification tasks [24]. A principal component analysis (PCA) is then applied to these multivariate observation vectors in each set, in order to reduce

their dimensions by fusing together highly collinear audio descriptors. Keeping only the first two PCA components, we use an SVM to compute a standard two-class confusion matrix within a standard cross-fold validation procedure to train/test the classifier. The confusion matrix shows the ways in which our classification model is confused when it makes predictions.

3) Other Regression Models on the Benchmark: To evaluate the performance of the O-R regression method, it is compared to two other models found in the literature.

a) Model: We used the logarithmic model from Vagle *et al.* [25]

$$\mathrm{W}_{ac} = \frac{10^{\mathrm{SPL}(8)/20} + 104.3}{53.91} \tag{5}$$

and the third-order model from Nystuen *et al.* [4]

$$\mathrm{W}_{ac} = 0.0005 * \mathrm{SPL}(8)^3 - 0.031 * \mathrm{SPL}(8)^2 + 0.4904 * \mathrm{SPL}(8) + 2.0871. \tag{6}$$

b) Calibration: As these conversion relationships are based on absolute sound levels, sensitivity bias, and instrument noise corrections are applied to acoustic data to make these models presumably "universal" (as stated by Ma *et al.* [2]) and insensitive to site-specific parameters. Such a correction is described in Ma *et al.* [2, Appendix A], and has been used in many subsequent studies [3], [4], [6], [7].

Generally, the W_{gt} data are used to identify periods of uniform wind (several hours of constant wind speed). Spectral data from each of these time periods are obtained, and the sound level at 8 kHz is adjusted to minimize the difference between W_{gt} and the acoustic wind speed W_{ac}. This value is the sensitivity offset for the particular passive acoustic sensor. The frequency-dependent component of the offset is obtained from the assumption that wind-generated spectra have known uniform SSs for moderate wind speed conditions from roughly 1 to 40 kHz [2], [25]. Note that this correction is small (usually less than 1 dB) with respect to the variability of the sound levels (tens of decibels).

4) Regression Model Performance: The full set of observations contains 40 000 snapshots, each of duration 10 s, after removal of contaminated (by acoustic sources other than wind) and near-surface snapshots (see Section II-A3). This data set was sorted into 10 stratified folds of 4000 observations each, and all models were evaluated using 10-fold cross validation. The stratified procedure applied to each data set means that each fold contains roughly the same proportions of observations from different wind speed classes that correspond to the Beaufort scale, and from different spatial areas that correspond to 10 space intervals along the complete glider route. Such stratified data partitioning is classically used to minimize risks of overfitting. Also, for training the proposed O-R regression model, we use one of the nine training folds in each split as a validation set for identifying the training epoch that yields the best model parameters when training with the remaining eight folds.

As an evaluation metric, we use the rms difference ϵ_{ws} between the ground truth and estimated wind speed. The average error $\overline{\epsilon_W}$ is then computed on the resulting errors in each fold, along with the median absolute deviation on these tests to assess the statistical significance of our experiments. We also compute the average relative error $\widetilde{\epsilon_W}$ in each fold, defined as the error percentage relative to the actual wind speed value being estimated.

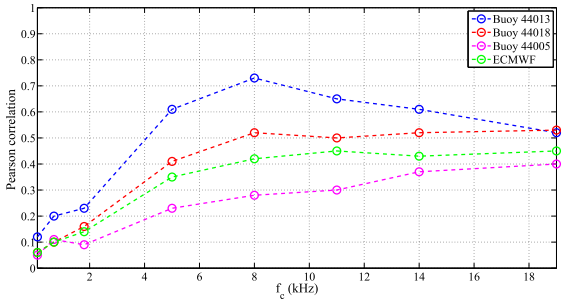

Fig. 2. Pearson correlation between the different wind speed measurements and the SPLs with their different center frequencies f_c.

TABLE III
PERFORMANCE OF DIFFERENT REGRESSION CLASSIFIERS TO ESTIMATE WIND SPEED. STANDARD DEVIATION OF EACH REGRESSION COEFFICIENT IS ALSO REPORTED

Classifiers	$\widetilde{\epsilon_W}$(± sd) (m.s^{-1})	$\widetilde{\epsilon_W}$(± sd) (%)	Ordinary R^2
Regression model by Vagle et al. [25]	3.5 (± 1.5)	27 (± 11)	53
Regression model by Nystuen et al. [4]	2.9 (± 1.1)	26 (± 5)	47
Proposed non-linear regression	2.3 (± 0.8)	19 (± 9)	61
Proposed O-R non-linear regression	**1.3 (± 0.7)**	**14 (± 7)**	**74**

III. RESULTS

A. Regression Model W_{ac} / W_{gt} ~SPL (f_c)

We first performed basic correlation and rms error analysis on two classical hypothesis found in the literature: 1) wind speed ground truth W_{gt} is the closest weather buoy from the glider trajectories and 2) the parameter f_c is set to 8 kHz. We compared wind speed of the closest National Oceanic and Atmospheric Administration (NOAA) buoy 44013 to other available wind speeds, and obtained rms errors of 2.5 m · s^{-1}, 3.2 m · s^{-1} and 5.1 m · s^{-1}, respectively, with ECMWF wind speed products, and the NOAA buoys 44018 and 44005. Also, Fig. 2 shows the Pearson correlation between the different wind speed measurements and the SPLs with their different center frequencies f_c. We can see that the highest correlation degree results from the linear equation $\mathrm{SPL}(8) \sim W_{44013}$, with a Pearson correlation of $r = 0.79$ (p-value < 0.001).

As listed in the first column of Table III, we tested four different regression classifiers, using the $SPL(8)$ as the single predictor. The first two are from Vagle *et al.* [25] and Nystuen *et al.* [4]. The last two correspond to our nonlinear regression models trained with *in situ* data, using the training data sets formed in each fold of the cross-validation procedure. The O-R model follows the relationship $\mathrm{W}_{ac} = 0.027418 * \mathrm{SPL}(f_c)^2 - 1.8705 * \mathrm{SPL}(f_c) + 37.9$. We can see that it is the O-R classifier that provides the best estimation performance of wind speed, with an average relative error $\widetilde{\epsilon_W}$ around 14%.

In Fig. 3, we superimposed the different regression models, where the outliers of the O-R regression one have been drawn in blue. We observe that outliers are mainly located

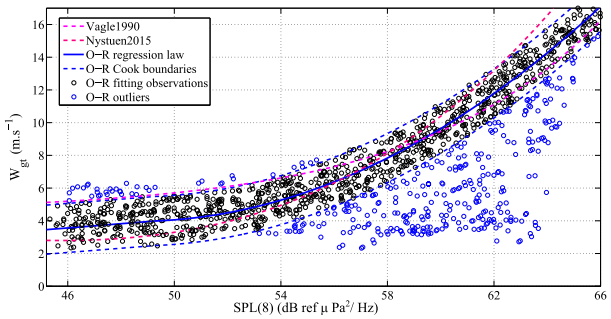

Fig. 3. O-R nonlinear regression model SPL(8) $\sim W_{44013}$ obtained from the training set of the second fold. Black circles: SPL(8) values of the acoustic snapshot that fit the O-R nonlinear regression model during a training fold of this model (i.e., from the WindObs observation class). Blue circles: outlier observations of this model (i.e., from the OutObs observation class).

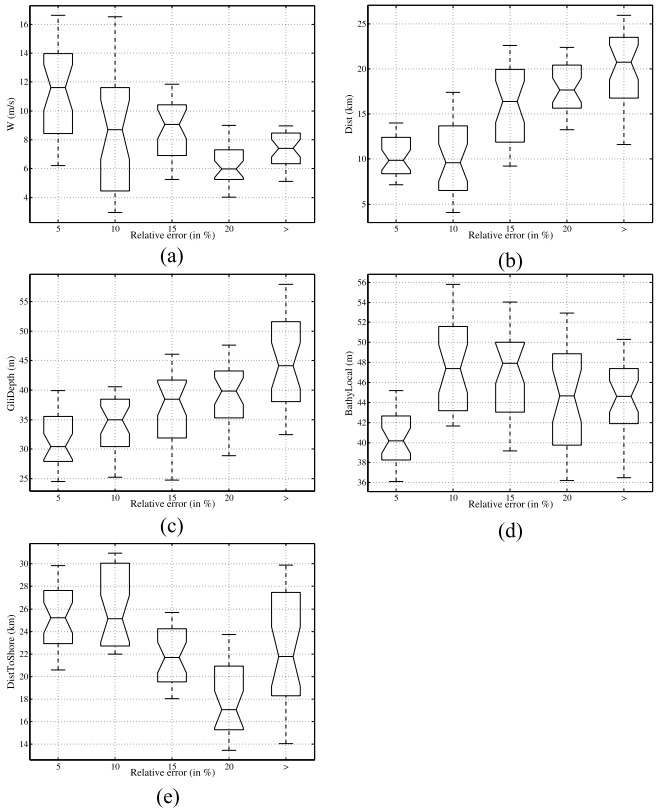

Fig. 4. $\widetilde{\epsilon_W}$ against different variables that could influence its distribution. (a) W_{44013}. (b) Dist. (c) GliDepth. (d) BathyLocal. (e) DistToShore.

on low values of wind speed, especially below 8 m $\cdot$ s^{-1}. The corresponding SPL(8) spans a large range of med to high values, from 55 to 65 dB. Consequently, low-wind-speed estimates exhibit a high rate of error estimation.

In Fig. 4, we represented the relative error of wind speed $\widetilde{\epsilon_W}$ against different variables that could influence its distribution, from top left to bottom right: W_{44013}, Dist, GliDepth, BathyLocal, DistToShore. Most significant variations of $\widetilde{\epsilon_W}$ are obtained for the variable W_{44013} (graph A).

To have the relative influence weight of each variable, we also performed a multilinear regression analysis using the regression equation $\widetilde{\epsilon_W} \sim \beta_0 + \beta_1 * W_{44013} + \beta_2 * \text{Dist} + \beta_3 * \text{GliDepth} + \beta_4 * \text{BathyLocal} + \beta_5 * \text{DistToShore}$, with results

TABLE IV

RESULTS ON THE MLR MODEL OF THE UNIVARIATE ERROR RESPONSE FOLLOWING THE MODEL $\widetilde{\epsilon_W} \sim \beta_0 + \beta_1 * W_{44013} + \beta_2 * \text{DIST} + \beta_3 * \text{GLIDEPTH} + \beta_4 * \text{BATHYLOCAL} + \beta_5 * \text{DISTTOSHORE}$. RESULTS ARE REPORTED IN TERMS OF REGRESSION COEFFICIENTS AND ORDINARY R^2. ALL NUMERICAL VALUES HAVE BEEN ROUNDED AT THE CLOSEST HUNDREDTH. MOST IMPORTANT REGRESSION COEFFICIENTS HAVE BEEN PUT IN BOLD

	Regression Coefficients β						Ordinary R^2 (in %)
	β_0	W_{44013}	Dist	GliDepth	BathyLocal	DistToShore	All
$\widetilde{\epsilon_W}$	0.07	**0.29**	0.13	0.1	0.08	0.09	81

TABLE V

AVERAGE CONFUSION MATRIX FOR THE TWO CLASSES: WINDOBS AND OUTOBS. 2000 SAMPLES ARE PRESENT IN EACH CLASS, AND A 10-FOLD CROSS VALIDATION PROCEDURE IS APPLIED. THE RESULTS REPORTED HERE ARE THE AVERAGES OF PERCENTAGES AND STANDARD DEVIATIONS RESPECTIVE TO EACH FOLD. TO IMPROVE READABILITY OF THE TABLE, HERE IS AN EXAMPLE: ON AVERAGE, 84% OF 2000 WIND OBSERVATIONS (I.E., 1680 OUT OF 2000 OBSERVATIONS FROM THE CLASS WINDOBS) ARE CORRECTLY RECOGNIZED AS WIND OBSERVATIONS, I.E., TP. WHILE 31% OF 2000 OUTLIER OBSERVATIONS (I.E., 620 OUT OF 2000 OBSERVATIONS FROM THE CLASS OUTOBS) ARE MISCLASSIFIED AS WIND OBSERVATIONS, I.E., ARE FALSE ALARMS

		Actual classes	
		WindObs	OutObs
Predicted classes by Nystuen et al. [4]	WindObs	65 ($\pm$ 16)	42 ($\pm$ 19)
	OutObs	35 ($\pm$ 9)	58 ($\pm$ 15)
Predicted classes by **PCA+SVM**	WindObs	**84 ($\pm$ 9)**	**31 ($\pm$ 11)**
	OutObs	16 ($\pm$ 2)	69 ($\pm$ 7)

shown in Table IV. Taken altogether, we confirm that W_{44013} is the most important explanatory variable for $\widetilde{\epsilon_W}$ variations, with the highest regression coefficient of 0.29. In other words, wind speed itself is the biggest driver of error for wind speed estimation.

B. Outlier Classification Performance

Table V shows the confusion matrix resulting from our PCA + SVM (see details Section II-C2.c) classification procedures, applied to the two sets Outliers and WindObs. The results are also compared with the method from Nystuen *et al.* [4, Appendix].

For the PCA + SVM algorithm, the first two principal components explained approximately 80% (first component, 55%; second component, 25%) of the total variable variance. This algorithm outperforms the Nystuen *et al.* [4, Appendix]'s algorithm, with an average rate of correct classification [i.e., True Positive (TP) in Receiver Operating Characteristic framework] of WindObs observations of 84%. False alarms, i.e., OutObs observations classified in the WindObs class, have an average rate of 31%.

Eventually, we want to put into relation this classification task of identifying OutObs with the one of wind speed estimation. Varying the Cook's distance modifies the absolute regression model, and consequently, the regression error $\widetilde{\epsilon_W}$. To look at how this may impact the classification performance metrics of TP and False Positives (FP), we plot in Fig. 5 the covariations of TP and FP against relative error $\widetilde{\epsilon_W}$. We can

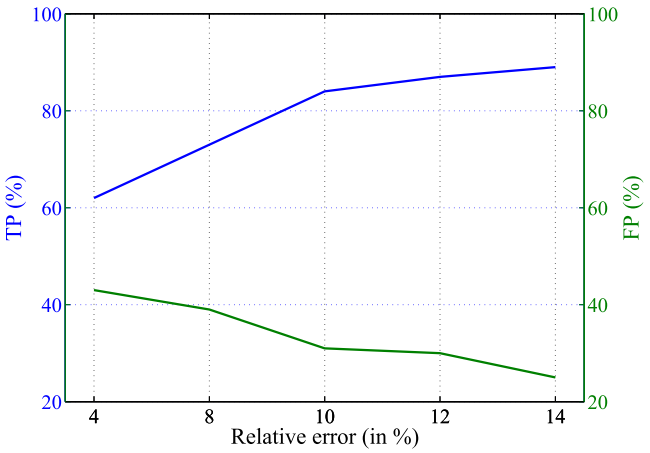

Fig. 5. Representation of covariations of TP and FP, both in%, against the relative error $\widetilde{\epsilon_W}$.

TABLE VI
TECHNICAL SPECIFICATIONS OF THE ACOUSTICAL METEOROLOGY SYSTEM

Technical characteristics	Definition	Value
W_{gt}	Ground truth of wind speed	NOAA buoy 44013
f_c	Central frequency of the third octave SPL used	8 kHz
$W_{ac} \sim SPL(f_c)$	Non-linear regression equation for wind speed estimation	$W_{ac} = 0.027418 * SPL(f_c)^2 - 1.8705 * SPL(f_c) + 37.9$
$W_{ac} \sim W_{gt}$	Linear regression equation for wind speed comparison with ground truth	$W_{ac} = 0 + 0.93 * W_{gt}$
$\epsilon_{\widetilde{W_{ac}}}$	Average relative error for wind speed estimation	14 ± 7 %
$\{TP; FP\}$	Classification performance of observations in regards to $SPL(f_c) \sim W_{gt}$	$\{84 \pm 9; 31 \pm 11)\}$%
τ	Execution time to process one 10-s observation snapshot with a standard laptop	$<<$ 3 ms

observe that enhancing classification performance is obtained by increasing the relative error $\widetilde{\epsilon_W}$.

C. Synthesis

In definitive, we resume in Table VI the technical specifications of the proposed acoustic-based wind speed estimation system, using the O-R regression model with *in situ* training.

IV. DISCUSSION

A. Wind Speed Ground Truth

For our experimental field of Massachusetts Bay, we have used two types of meteorological sources, namely, reassimilation models and weather buoys. It is known that for both satellite and reanalysis data, the highest errors in wind velocity, in comparison to contact measurements, are observed for extreme values, i.e., with overestimation under weak winds ($W < 4$ m $\cdot$ s^{-1}) and underestimation under strong winds ($W > 12$ m $\cdot$ s^{-1}). The fact that errors increase for scatterometer measurements under very weak winds is known [26], [27]. High errors in determining the direction and velocity of wind under weak winds are associated with the insufficient strength of signal received by satellite. Globally, Garmashov *et al.* [27] reported that reanalysis data have an average rms deviation in the velocity amplitude that varies from 1.9 to 2.2 m $\cdot$ s^{-1}.

In our study, when comparing ECMWF wind speed products to the NOAA buoy 44013, an rms deviation of 2.5 m $\cdot$ s^{-1} was observed. Consequently, reanalysis data and satellite imagery might be an error-prone ground truth for wind speed, especially when used in coastal environments where satellite-based estimations seem to be less accurate [28]. This needs to be carefully taken into account in acoustical meteorology, where some studies exclusively rely on satellite imagery, e.g., Tropical Rainfall Measuring Mission and QwikScat in Riser *et al.* [5], for rainfall and winds, respectively.

Also, rms deviations of 3.2 m $\cdot$ s^{-1} and 5.1 m $\cdot$ s^{-1} were observed between the NOAA buoy 44013 and the NOAA buoys 44018 and 44005, respectively. These differences correspond to local variations in wind speed, which are noticeable even at a 40-km distance (distance between buoys 44013 and 44018). This highlights the importance of selecting a buoy as close as possible to the acoustic recorder. In the literature, average distances between recorders and buoys (or onshore meteorological stations) vary from 40 km [19] to 80 km [20]. In our study, maximum time and space intervals between the glider and buoy 44013 were 1 h and 24 km. These intervals are sufficiently small so that one can expect that errors associated with the spatiotemporal disagreement of data are relatively small.

A multilinear regression model was used to see which meteorological variables best explain the multivariate acoustic response composed of eight SPLs in different frequency bands. From this analysis, we showed that the highest correlation is obtained with the buoy 44013, which is the closest to the glider. Correlations with farther buoys and reanalysis data are poorer. This highlights the importance of correctly choosing the ground truth to calibrate the acoustical meteorology in a coastal environment. Interestingly, the SPL with the highest correlation is always SPL(8), whatever ground truth is considered. This corresponds to the very frequency adopted by past research studies [25], [29], and validated for different marine environments [2], [4], [6].

B. Empirical Conversion Relationships

Based on the wind speed ground truth W_{gt}, we have trained a nonlinear regression model with SPL(8) as a single-feature predictor. For low wind speed values, and in the absence of concurrent acoustic sources, the ocean bottom noise floor level should be measured. However, as observed in Fig. 3, OutObs mostly overestimates wind speed, suggesting that acoustic energy is produced by sources other than wind speed. When wind speed increases, the decreasing amount of OutObs suggests that these sources become less and less significant to the overall sound budget.

It is interesting to compare our obtained regression model to other ones published in the literature, which can vary significantly, depending on the different experimental configurations. These models can be linear [19], logarithmic [2], [3], quadratic [20], or third-order polynomial [4]. However, note that comparison of different wind speed estimation algorithms are quite rare in the literature, excepting in Pensieri *et al.* [30, Fig. 10] and Pensieri *et al.* [20, Fig. 14], where drastic differences are observed in comparison to other models [25], [31], [32]. The largest intermodel differences observed in our

own study, between our O-R model, and Vagle *et al.* [25] and Nystuen *et al.* [4] ones, were at extreme values, especially the lowest ones under 6 $\mathrm{m} \cdot \mathrm{s}^{-1}$, which has been confirmed by other studies (e.g., [4, Fig. 9]).

In definitive, as suggested by Yang *et al.* [6], *in situ* calibration of passive acoustics sensors is the most promising solution to reduce errors in wind speed estimation. In our study, making our regression model robust to outliers reduced significantly the average relative estimation error, from 2.3 $\mathrm{m} \cdot \mathrm{s}^{-1}$ to 1.3 $\mathrm{m} \cdot \mathrm{s}^{-1}$ (Table V). Unfortunately, the literature in acoustical meteorology does not provide a clear baseline reference for errors in wind speed estimation. We can mention that Pensieri *et al.* [30] obtained their highest error for the Beaufort class F1 (low wind speed), and an approximate error of 1 $\mathrm{m} \cdot \mathrm{s}^{-1}$ for the higher class F7, which are both consistent with our results.

Also, the potential effects of several environmental factors on noise levels were examined to assess how they influence the wind dependence of spectral levels. In particular, to develop more efficient classification systems, it is also interesting to investigate the physical origins of OutObs observations, i.e., corresponding to the outliers identified in our O-R regression models. Different comments can be made based on the different graphs shown in Fig. 4 and Table IV, that represent the impacts of different variables on the distribution of $\widetilde{\epsilon_W}$. As already seen, wind speed W_{gt} is very influential (graph A), exhibiting a decreasing exponential relation with the dispersion and average values of $\widetilde{\epsilon_W}$. Indeed, wind speed estimation with passive acoustic monitoring is harder for low wind speed than for higher wind speed for at least two reasons. First of all, when the wind speed is less than 5 m/s, there is very little wave breaking at the ocean surface, and thus, there is very little for an acoustic wind speed measurement [3]. Also, the weak acoustic signal created by low wind speed is easily masked by other acoustic sources, leading to a signal-to-noise ratio issue. As a result, a higher number of outliers is present for low wind speed values (as can be seen in Fig. 3), which leads to higher estimation errors (see graph A shown in Fig. 4).

For the influence variable Dist (graph B), the slight increase of the relative error $\widetilde{\epsilon_W}$ with the distance Dist suggests that this error may reflect a spatial change of wind condition, rather than an estimation error. In other words, at the glider position, the acoustical wind speed estimate may be more accurate than the distant buoy measurement. Variations in GliDepth (graph C) and BathyLocal (graph D) have more marginal impacts on $\widetilde{\epsilon_W}$, although large errors (more than 20%) occur mostly when the glider is deeper than 40 m. Cauchy *et al.* [19] reported depth-related errors less than 0.5 $\mathrm{m} \cdot \mathrm{s}^{-1}$ in deep waters. Last but not least, $\widetilde{\epsilon_W}$ shows a stronger dependence on DistToShore (graph E), that may be explained by a reinforcement of concurrent nonmeteorological sources when approaching the coast (e.g., crashing waves).

C. Outlier Classification Performance

Most acoustical meteorology studies take place in underwater soundscapes with minimal polluting sources [33]. Some researchers also manually preprocessed their recordings to remove contaminated observations, as in Pensieri *et al.* [30], where spectra related to rain events detected by a pluviometer onboard a buoy were discarded as well as spectra corresponding to ship passage within 15 min. Similarly, in most shallow water studies, data contaminated by traffic noise and/or marine mammal sounds are excluded from the analysis when studying the wind dependence of ambient noise [3], [13], [34], [35]. In our study, the marine environment of Massachusetts Bay during winters presents a complex soundscape with multiple sources concurrent to the wind. In particular, rainfall has been shown to highly complicate wind speed estimation [2]. Also, the intermittent proximity of gliders to large vessels, crashing waves, singing humpback whales could have contaminated wind observations.

Ma *et al.* [2, Appendix B] described a classification framework of underwater acoustic sources based on multivariate classification tests with thresholded absolute levels, which has been used in many subsequent studies [3], [4], and also implemented on board ARGO profilers [5]–[7]. This framework is based on the following steps and hypothesis [36].

1) Only a few spectral parameters are needed to identify most sound sources.
2) Multivariate classification algorithms are applied on board the float.
3) Once classified, wind speed and rainfall rate are quantified. This includes highly site-specific heuristic rules such as assuming that concurrent acoustic source is bounded into specific frequency bands. This is unfortunately hard to generalize for global scale acoustical monitoring, which motivates the need for an automatic classification of data containing wind noise only, versus data contaminated by other sound sources.

In our study, a data-driven classification framework was designed to address this issue. The O-R model provides a rich training data set to first characterize acoustically these OutObs and then evaluate classification performance in automatically identifying them. In comparison to the classification algorithm proposed in Ma *et al.* [2, Appendix B], our SVM + PCA method provided the best results in recognizing both wind-generated and nonwind noises (TP $\approx$ 84% and FP $\approx$ 31%, see Table V). The performance gain can be explained by the *in situ* training of more flexible audio features. Also, our longer analysis time windows of 10 s, in comparison to the 10 ms commonly found in the literature, probably captures more efficiently the signatures of different acoustic events, thanks to the use of the time-dependent features.

Fig. 5 reveals the tradeoff that exists in the global system between efficient wind speed estimation (i.e., low values of $\widetilde{\epsilon_W}$) and efficient outlier rejection (i.e., high values in TP and low values in FP). To further enhance classification performance, and eventually fully validate mobile acoustical weather systems for operational use, more sophisticated machine learning and source separation methods will need to be explored. The calibration of the acoustic systems will likely require a systematic recovering of raw acoustic data, which is difficult to achieve in practice. Also, it will be important to collect longer-term measurements on large areas and to compare acoustic estimates with other meteorological sources.

Complementary observations on the spatiotemporal distribution of nonmeteorological competitive acoustic sources (e.g., biological surveys from ships) specific to each deployment site will also be necessary.

V. Conclusion

This paper reports results on the use of an underwater glider to perform acoustical meteorology. It takes the form of a methodological protocol to deploy an operational acoustic-based *in situ* wind speed estimation system, especially by providing technical specifications that inform us of its performance. This protocol paves the way toward the development of an operational glider-embedded wind speed estimation system.

The long-term goal of this paper is to use passive acoustic remote sensing of the marine environment as a standard measurement technique for observing air–sea interaction processes. Such sampling platforms could have a direct application in marine meteorology as contact measurements distributed at large scale to calibrate satellite products.

Acknowledgment

The authors would like to thank their collaborators, namely, NOAA Northeast Fisheries Science Center, The Nature Conservancy, Stellwagen Bank National Marine Sanctuary, Massachusetts Division of Marine Fisheries, and the University of Massachusetts Dartmouth.

References

[1] J. A. Nystuen, "Rainfall measurements using underwater ambient noise," *J. Acoust. Soc. Amer.*, vol. 79, no. 4, pp. 972–982, 1986.

[2] B. B. Ma and J. A. Nystuen, "Passive acoustic detection and measurement of rainfall at sea," *J. Atmos. Ocean. Technol.*, vol. 22, pp. 1225–1248, Aug. 2005.

[3] J. A. Nystuen, S. E. Moore, and P. J. Stabeno, "A sound budget for the southeastern Bering Sea: Measuring wind, rainfall, shipping, and other sources of underwater sound," *J. Acoust. Soc. Amer.*, vol. 128, no. 1, pp. 58–65, 2010.

[4] J. A. Nystuen, M. A. Anagnostou, E. M. Anagnostou, and A. Papadopoulos, "Monitoring Greek seas using passive underwater acoustics," *J. Atmos. Ocean. Technol.*, vol. 32, pp. 334–349, Feb. 2015.

[5] S. C. Riser, J. A. Nystuen, and A. Rogers, "Monsoon effects in the Bay of Bengal inferred from profiling float-based measurements of wind speed and rainfall," *Limnol. Oceanogr.*, vol. 53, no. 5, pp. 2080–2093, 2008.

[6] J. Yang, S. C. Riser, J. Nystuen, W. E. Asher, and A. T. Jessup, "Regional rainfall measurements using the passive aquatic listener during the SPURS field campaign," *Oceanography*, vol. 28, no. 1, pp. 124–133, Mar. 2015.

[7] J. Yang, W. E. Asher, and S. C. Riser, "Rainfall measurements in the North Atlantic Ocean using underwater ambient sound," in *Proc. IEEE/OES China Ocean Acoust. Symp.*, Jan. 2016, pp. 1–4.

[8] D. Cazau, J. Bonnel, J. Jouma'a, Y. le Bras, and C. Guinet, "Measuring the marine soundscape of the indian ocean with southern elephant seals used as acoustic gliders of opportunity," *J. Atmos. Ocean. Technol.*, vol. 34, pp. 207–223, Jan. 2017.

[9] D. L. Rudnick, R. E. Davis, C. C. Eriksen, D. M. Fratantoni, and M. J. Perry, "Underwater gliders for ocean research," *Marine Technol. Soc. J.*, vol. 34, no. 2, pp. 48–59, 2004.

[10] J. A. Nystuen, "Acoustical rainfall analysis: Rainfall drop size distribution using the underwater sound field," *J. Atmos. Ocean. Technol.*, vol. 13, pp. 74–84, Feb. 1996.

[11] C. L. Piggott, "Ambient sea noise at low frequencies in shallow water of the scotian shelf," *J. Acoust. Soc. Amer.*, vol. 36, no. 11, pp. 2152–2163, 1964.

[12] D. D. Lemon, D. M. Farmer, and D. R. Watts, "Acoustic measurements of wind speed and precipitation over a continental shelf," *J. Geophys. Res.*, vol. 89, no. C3, pp. 3462–3472, May 1984.

[13] S. Ramji, G. Latha, V. Rajendran, and S. Ramakrishnan, "Wind dependence of ambient noise in shallow water of Bay of Bengal," *Appl. Acoust.*, vol. 69, no. 12, pp. 1294–1298, Dec. 2008.

[14] V. O. Knudsen, R. S. Alford, and J. W. Emling, "Underwater ambient noise," *J. Marine Res.*, vol. 7, pp. 410–429, 1948.

[15] D. Mathias, C. Gervaise, and L. Di Oro, "Wind dependence of ambient noise in a biologically rich coastal area," *J. Acoust. Soc. Amer.*, vol. 139, no. 2, pp. 839–850, 2016.

[16] W. A. Kuperman and M. C. Ferla, "A shallow water experiment to determine the source spectrum level of wind-generated noise," *J. Acoust. Soc. Amer.*, vol. 77, no. 6, pp. 2067–2073, 1985.

[17] F. Ingenito and S. N. Wolf, "Site dependence of wind-dominated ambient noise in shallow water," *J. Acoust. Soc. Amer.*, vol. 85, no. 1, pp. 141–145, 1989.

[18] D. E. Weston and P. A. Ching, "Wind effects in shallow-water acoustic transmission," *J. Acoust. Soc. Amer.*, vol. 86, no. 4, pp. 1530–1545, 1989.

[19] P. Cauchy, P. Testor, L. Mortier, L. Beguery, and M.-N. Bouin, "Passive acoustics embedded on gliders—Weather observation through ambient noise," in *Proc. 3rd Underwater Acoust. Conf. Exhib. (UACE)*, 2015, pp. 565–570

[20] S. Pensieri, R. Bozzano, J. A. Nystuen, E. N. Anagnostou, M. N. Anagnostou, and R. Bechini, "Underwater acoustic measurements to estimate wind and rainfall in the mediterranean sea," *Adv. Meteorol.*, vol. 2015, Mar. 2015, Art. no. 612512.

[21] P. Berrisford *et al.*, *The Era-Interim Archive Version 2.0*. Reading, MA, USA: Shinfield Park, 2011.

[22] J. A. Nystuen, E. Amitai, E. N. Anagnostou, and M. N. Anagnostou, "Spatial averaging of oceanic rainfall variability using underwater sound," Appl. Phys. Lab., Univ. Washington Tacoma, Tacoma, WA, USA, Tech. Rep. APL-UW TR 0701, 2007.

[23] K. A. Bollen and R. W. Jackman, "Regression diagnostics: An expository treatment of outliers and influential cases," in *Modern Methods of Data Analysis*, J. Fox and J. S. Long, Eds. Newbury Park, CA, USA: Sage, 1990, pp. 91–257.

[24] G. Peeters, B. L. Giordano, P. Susini, N. Misdariis, and S. McAdams, "The timbre toolbox: Extracting audio descriptors from musical signals," *J. Acoust. Soc. Amer.*, vol. 130, no. 5, pp. 2902–2916, 2011.

[25] S. Vagle, W. G. Large, and D. M. Farmer, "An evaluation of the WOTAN technique of inferring oceanic winds from underwater ambient sound," *J. Atmos. Ocean. Technol.*, vol. 7, pp. 576–595, Aug. 1990.

[26] W. J. Plant, "Effects of wind variability on scatterometry at low wind speeds," *J. Geophys. Res.*, vol. 105, no. C7, pp. 16899–16910, 2000.

[27] A. V. Garmashov, A. A. Kubryakov, M. V. Shokurov, S. V. Stanichny, Y. N. Toloknov, and A. I. Korovushkin, "Comparing satellite and meteorological data on wind velocity over the Black Sea," *Izvestiya, Atmos. Ocean. Phys.*, vol. 52, no. 3, pp. 309–316, May 2016.

[28] P. M. Ruti, S. Marullo, F. D'Ortenzio, and M. Tremant, "Comparison of analyzed and measured wind speeds in the perspective of oceanic simulations over the Mediterranean basin: Analyses, QuikSCAT and buoy data," *J. Marine Syst.*, vol. 70, nos. 1–2, pp. 33–48, 2008.

[29] J. A. Nystuen, "Listening to raindrops from underwater: An acoustic disdrometer," *J. Atmos. Ocean. Technol.*, vol. 18, pp. 1640–1657, Oct. 2001.

[30] S. Pensieri, R. Bozzano, M. Anagnostou, E. Anagnostou, R. Bechini, and J. Nystuen, "Monitoring the oceanic environment through passive underwater acoustics," in *Proc. MTS/IEEE OCEANS-Bergen*, Jun. 2013, pp. 1–10.

[31] J. A. Nystuen, "Quantifying physical processes in the marine environment using underwater sound," in *Proc. IACM UAM*, Kos, Greece, Jun. 2011, pp. 20–24.

[32] M. N. Anagnostou, J. A. Nystuen, E. N. Anagnostou, A. Papadopoulos, and V. Lykousis, "Passive aquatic listener (PAL): An adoptive underwater acoustic recording system for the marine environment," *Nucl. Instrum. Methods Phys. Res. A, Accel. Spectrom. Detect. Assoc. Equip.*, vols. 626–627, pp. S94–S98, Jan. 2011.

[33] D. B. Reeder, E. S. Sheffield, and S. S. Mach, "Wind-generated ambient noise in a topographically isolated basin: A pre-industrial era proxy," *J. Acoust. Soc. Amer.*, vol. 129, no. 1, pp. 64–73, 2011.

[34] M. A. McDonald, J. A. Hildebrand, S. M. Wiggins, and D. Ross, "A 50 Year comparison of ambient ocean noise near San Clemente Island: A bathymetrically complex coastal region off Southern California," *J. Acoust. Soc. Amer.*, vol. 124, no. 4, pp. 1985–1992, 2008.

[35] A. Poikonen and S. Madekivi, "Wind-generated ambient noise in a shallow brackish water environment in the archipelago of the Gulf of Finland," *J. Acoust. Soc. Amer.*, vol. 127, no. 6, pp. 3385–3393, 2010.

[36] J. A. Nystuen, S. C. Riser, T. Wen, and D. Swift, "Interpreted acoustic ocean observations from Argo floats," *J. Acoust. Soc. Amer.*, vol. 129, no. 4, p. 400, 2011.

Dorian Cazau received the Ph.D. degree in acoustics and signal processing from Pierre-and-Marie-Curie University, Paris, France, in 2012

In 2012, he held a post-doctoral position at ENSTA Bretagne, Brest, France. He is currently a French Post-Doctoral Researcher with the Institut Mines Telecom Atlantique, Lab-STICC, UMR CNRS 6285, where he is involved in acoustic data analysis. He is involved in computer analysis of audio signals, combining methods from physical acoustics, signal processing, statistical modeling, and machine learning. His research interests include different interdisciplinary application fields, including environmental acoustics, bioacoustics, and acoustical oceanography.

Julien Bonnel (S'08–M'11) received the Ph.D. degree in signal processing from the Grenoble Institut National Polytechnique, Grenoble, France, in 2010.

From 2010 to 2017, he was an Assistant Professor with ENSTA Bretagne, Lab-STICC, UMR CNRS 6285, Brest, France. Since 2017, he has been an Associate Scientist with the Woods Hole Oceanographic Institution, Falmouth, MA, USA. His research interests include signal processing and underwater acoustics, particularly time–frequency analysis, source detection/localization, geoacoustic inversion, acoustical tomography, passive acoustic monitoring, and bioacoustics.

Dr. Bonnel is a member of the Acoustical Society of America.

Mark Baumgartner was born in Albany, NY, USA, in 1968. He received the B.S. degree in mathematics and computer science from the University of Notre Dame, Notre Dame, IN, USA, in 1990, the M.S. degree in marine science from the University of Southern Mississippi, Hattiesburg, MS, USA, in 1995, and the Ph.D. degree in biological oceanography from Oregon State University, Corvallis, OR, USA, in 2002.

He was a Post-Doctoral Scholar with the Woods Hole Oceanographic Institution, Falmouth, MA, USA, where he was a Scientific Staff in 2005. He is currently an Associate Scientist with the Department of Biology, Woods Hole Oceanographic Institution. He is involved in the study of the ecology of top marine predators, particularly baleen whales, and mesozooplankton with a variety of approaches, including passive acoustics, tagging, zooplankton instrumentation, and autonomous platforms.